Linear-quadratic-Gaussian Control of Line Active-power Flow

Abdullah Al-Digs
Department of Electrical
and Computer Engineering
The University of British Columbia
Vancouver, BC V6T 1Z4
Email: aldigs@ece.ubc.ca

Sairaj V. Dhople
Department of Electrical
and Computer Engineering
University of Minnesota
Minneapolis, MN 55455
Email: sdhople@umn.edu

Yu Christine Chen
Department of Electrical
and Computer Engineering
The University of British Columbia
Vancouver, BC V6T 1Z4
Email: chen@ece.ubc.ca

***Abstract*—The existing transmission network is becoming increasingly overloaded due to rapidly growing electricity demand, deregulation, and limited investment in transmission network expansion. This paper presents a state-space model-based control design for regulating line active-power flows in AC electric power systems using linear-quadratic-Gaussian (LQG) control. At its core, the proposed method relies on the linear mapping of nodal active- and reactive-power injections to active-power line flows. Building on this, we outline a combined linear-quadratic regulator and Kalman-filter design to optimally dispatch generators and controllable loads to maintain line flows while ensuring power balance. We demonstrate the utility of the proposed LQG controller with a representative congestion-management application.**

I. Introduction

This paper presents a design strategy for line active-power flow tracking using linear-quadratic-Gaussian (LQG) control in a power system operating in sinusoidal steady state. We study the bulk AC power-system setting, where synchronous generators serve constant-power loads through a connected, linear time-invariant electrical network. More precisely, Π-equivalent circuit models are adopted for the lines, shunt elements are composed of linear circuit components, and a subset of these nodes have constant active- and reactive-power injections. With rapidly growing electricity demand and increased penetration of distributed generation, there is definitely an impetus to expand the existing transmission network. However, expanding the power system network is hindered by economic and environmental constraints [1]. As a result, transmission lines may operate in an overloaded state (i.e., above their thermal limits) [2]. In light of this, effective methods to control line active-power flows are necessary to optimize the utilization of existing resources, e.g., generation and transmission capacities, while maintaining reliable and secure operation of the network.

Traditionally, line-flow control has been realized through decentralized hardware-based control using, e.g., distributed static series compensators (DSSCs) [3], phase shifting transformers (PSTs) [4], flexible AC transmission system (FACTS) controllers [2], and unified power flow controllers (UPFCs) [1]. While these solutions require little-to-no communication, installing them ubiquitously is economically prohibitive and it increases system complexity. Furthermore, they do not adapt to short-term contingencies and future system modifications [5]. On the other hand, global line-flow control is performed as part of the automatic generation control (AGC) system, which maintains scheduled inter-area tie-line flows by ensuring that each control area balances its own net load [6].

Given the prevalent competitive electricity environment, line active-power flow control is potentially useful in a variety of settings to ensure that the system is operated efficiently and fairly. Examples include congestion management, AGC, eliminating redundant loop flows, etc. Steering clear of specific power-system applications, in this paper, we propose a method to determine nodal active-power injections to yield optimal line active-power flow trajectories that eventually converge to the desired reference values. As the system conditions fluctuate and the operating point varies, the controller systematically introduces small-signal modifications to generator and controllable-load active-power setpoints based on the sensitivities of line flows with respect to nodal injections, while accounting for relative costs of individual injections.

The proposed controller is an LQG controller that includes a linear-quadratic regulator (LQR) that guarantees robustness and optimal tracking regardless of initial conditions; and it incorporates an optimal estimator, namely the Kalman filter, which accounts for random measurement and system disturbances. The proposed controller is unique from two perspectives. First, from a modelling perspective, the proposed method relies on a linear mapping of nodal active- and reactive-power injections to active-power line flows that significantly simplifies controller synthesis while maintaining sufficient accuracy to achieve the control aim. Second, from a control perspective, the controller ensures that system active-power balance is maintained at all times, and this is accomplished with a non-standard LQR cost function that guarantees the elimination of nodal active-power injection imbalances at each time step. In order to verify the proposed control method, time-domain simulations are conducted to mimic the dynamic behaviour of the system considering synchronous machine dynamics. We demonstrate the effectiveness of the controller to track desired line-flow references using synthetic measurements periodically sampled from the time-domain simulation.

II. Preliminaries

In this section, we describe the power system network. Using an exact linear mapping of nodal active- and reactive-power injections to line active-power flows, we develop a discrete-time system to be used for control synthesis.

A. Network Description

Consider an AC electric power network with N nodes collected in the set $\mathcal{N}$ operating in sinusoidal steady state. The set of transmission lines is represented by $\mathcal{E} := \{(m,n)\} \subseteq \mathcal{N} \times \mathcal{N}$. Each line is modelled using the lumped-parameter Π-model with series admittance $y_{mn} \in \mathbb{C}$ and shunt admittance $y^{\text{sh}}_{mn} \in \mathbb{C}$. Then, the entry in the mth row and nth column of the network admittance matrix, denoted by Y, is specified as

$$[Y]_{mn} := \begin{cases} y_m + \sum_{(m,k)\in\mathcal{E}} y_{mk}, & \text{if } m = n, \\ -y_{mn}, & \text{if } (m,n) \in \mathcal{E}, \\ 0, & \text{otherwise}, \end{cases} \tag{1}$$

where $y_m = g_m + \mathrm{j}b_m := y_{mm} + \sum_{k\in\mathcal{N}_m} y^{\text{sh}}_{mk}$ denotes the total shunt admittance connected to node m, $\mathcal{N}_m \subseteq \mathcal{N}$ represents the set of neighbours of node m, and $y_{mm} \in \mathbb{C}$ captures any passive shunt elements connected to node m. Since our goal is to synthesize controllers aided by measurements of electrical signals, we introduce the discrete-time index, $k \in \mathbb{Z}_{\geq 0}$ which denotes time instants when the physical system is probed or actuated. With this in mind, let $V_i[k] = |V_i[k]|\angle\theta_i[k] \in \mathbb{C}$ represent the voltage phasor at node i at time instants $k \in \mathbb{Z}_{\geq 0}$; similarly, let $I_i[k] \in \mathbb{C}$ denote the current injected into node i at time instants $k \in \mathbb{Z}_{\geq 0}$. Furthermore, collect steady-state nodal voltage phasors into the vector $V[k] = [V_1[k], \ldots, V_N[k]]^{\mathrm{T}}$ and current injections into $I[k] = [I_1[k], \ldots, I_N[k]]^{\mathrm{T}}$. Then, at time instant k, applying Kirchhoff's current law at each node and combining them into matrix-vector form, the current balance can be compactly represented as

$$I[k] = YV[k]. \tag{2}$$

Denote the vector of complex-power nodal injections at time instant k by $S[k] = [S_1[k], \ldots, S_N[k]]^{\mathrm{T}} = P[k] + \mathrm{j}Q[k]$, with $P[k] = [P_1[k], \ldots, P_N[k]]^{\mathrm{T}}$ and $Q[k] = [Q_1[k], \ldots, Q_N[k]]^{\mathrm{T}}$. (By convention, $P_i[k]$ and $Q_i[k]$ are positive for generation and negative for loads.) Then, complex-power nodal injections can be compactly written as

$$S[k] = \operatorname{diag}(V[k])\, I[k]^*, \tag{3}$$

where $\operatorname{diag}(V[k])$ denotes a diagonal matrix formed with entries of the vector $V[k]$.

B. Network Line Flows

Next, shifting our focus from nodal injections to line flows, we can express the current flowing in line $(m,n) \in \mathcal{E}$ at time instant k as

$$I_{(m,n)}[k] = \left(y_{mn} e_{mn}^{\mathrm{T}} + y^{\text{sh}}_{mn} e_m^{\mathrm{T}}\right) Y^{-1} I[k] =: \kappa_{(m,n)}^{\mathrm{T}} I[k], \tag{4}$$

where $\kappa_{(m,n)} \in \mathbb{C}^N$ are the current injection sensitivity factors and $e_m \in \mathbb{R}^N$ denotes a column vector of all zeros except with the m-th entry equal to 1, and $e_{mn} := e_m - e_n$.

Denote, by $S_{(m,n)}[k] = P_{(m,n)}[k] + \mathrm{j}Q_{(m,n)}[k]$, the complex power flowing across line (m,n). We can write

$$S_{(m,n)}[k] = V_m[k] I^*_{(m,n)}[k]. \tag{5}$$

Further, decompose the current injection sensitivity factors from (4) into real and imaginary components as

$$\kappa_{(m,n)} = \alpha_{(m,n)} + \mathrm{j}\beta_{(m,n)}.$$

Leveraging the above decomposition, substituting the current injection sensitivity factors from (4) into (5), and defining $\theta^m := \theta_m \mathbb{1}_N - \theta$ ($\mathbb{1}_N$ is an N-dimensional column vector with all entries equal to 1), we obtain [7]

$$P_{(m,n)}[k] = \Phi^P_{(m,n)}[k] P[k] + \Phi^Q_{(m,n)}[k] Q[k], \tag{6}$$

where

$$\Phi^P_{(m,n)}[k] = |V_m[k]| u^{\mathrm{T}}_{(m,n)}, \tag{7}$$

$$\Phi^Q_{(m,n)}[k] = -|V_m[k]| v^{\mathrm{T}}_{(m,n)}, \tag{8}$$

with $u_{(m,n)}, v_{(m,n)} \in \mathbb{R}^N$ given by

$$u_{(m,n)} = \operatorname{diag}\left(\frac{\cos\theta^m}{|V|}\right)\alpha_{(m,n)} + \operatorname{diag}\left(\frac{\sin\theta^m}{|V|}\right)\beta_{(m,n)}, \tag{9}$$

$$v_{(m,n)} = \operatorname{diag}\left(\frac{\sin\theta^m}{|V|}\right)\alpha_{(m,n)} - \operatorname{diag}\left(\frac{\cos\theta^m}{|V|}\right)\beta_{(m,n)}. \tag{10}$$

Above, $\operatorname{diag}(x/y)$ denotes a diagonal matrix with the mth entry given by x_m/y_m, where x_m and y_m are the mth entries of vectors x and y, respectively. The expression in (6) reveals the contribution of each nodal injection to the net active-power flow in line (m,n). The mapping between active-power flows and active- and reactive-power injections is established and fully derived in [7]. Note that the parametrization of voltage magnitudes and phases in terms of $[k]$ is dropped in (9) and (10) to contain notational burden.

For subsequent discussions, we will assume that we are interested in controlling the active-power flows on E lines. Collecting these from (6), we write

$$P_{(m,n)}[k] = \Phi_P[k] P[k] + \Phi_Q[k] Q[k], \tag{11}$$

where (with a slight abuse of notation) $P_{(m,n)} \in \mathbb{R}^E$ collects the active-power flows of interest, and $\Phi_P[k]$, $\Phi_Q[k] \in \mathbb{R}^{E\times N}$ are constructed appropriately from (7) and (8), respectively.

C. State-space Model

With respect to the network described above, consider small variations in nodal active- and reactive-power injections $\Delta P[k] = P[k+1] - P[k]$ and $\Delta Q[k] = Q[k+1] - Q[k]$, respectively. Using (11), the effect of these small variations on $P_{(m,n)}$ can be approximated as

$$\begin{aligned} P_{(m,n)}[k+1] = {} & \Phi_P[k]\left(P[k] + \Delta P[k]\right) \\ & + \Phi_Q[k]\left(Q[k] + \Delta Q[k]\right), \end{aligned} \tag{12}$$

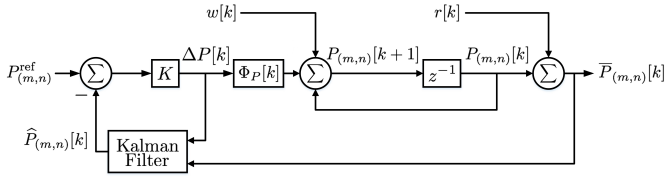

Fig. 1: Block diagram for the closed-loop control system.

which yields the following recurrence relation:

$$P_{(m,n)}[k+1] = P_{(m,n)}[k] + \Phi_P[k]\Delta P[k] + w[k], \quad (13)$$

where $w[k] = \Phi_Q[k]\Delta Q[k]$ represents a *bounded* external disturbance due to changes in reactive-power injections that arise either naturally in the system or due to (coupling with) active-power injection variations. In either case, we do not exercise any control over it. We are interested in regulating network active-power line flows to desired setpoints despite uncontrolled variations in reactive power. Specifically, our goal is to optimally track the line flows $P_{(m,n)}[k] \in \mathbb{R}^E$ to some reference $P^{\text{ref}}_{(m,n)} \in \mathbb{R}^E$ using $\Delta P[k] \in \mathbb{R}^N$ as the control input while satisfying power balance. In subsequent discussions, we assume that we do not have access to perfect measurements of the line flows. Particularly, our measurements take the form

$$\overline{P}_{(m,n)}[k] = P_{(m,n)}[k] + r[k], \quad (14)$$

where $r[k] \in \mathbb{R}^E$ is a bounded vector that captures measurement noise.

We close this section with a few remarks on the stability, controllability, and observability of the system in (13)–(14). For a discrete-time (DT) system to be stable, its eigenvalues must lie within the unit disc of the complex plane. The system model in (13) is marginally stable with eigenvalues on the boundary of the unit disc. We also find that (13) is controllable by checking that its controllability matrix has full row rank. Finally, with the output of the system as $\overline{P}_{(m,n)}[k]$, the system in (13)–(14) is observable since its observability matrix has full column rank. With these properties satisfied, next, we describe the design of a linear-quadratic-Gaussian (LQG) controller to achieve optimal tracking of $P_{(m,n)}$ to $P^{\text{ref}}_{(m,n)}$.

III. Control Design

In this section, we propose to use an LQG controller to achieve optimal tracking of line active-power flows while contending with measurement noise as well as errors arising from reactive-power couplings. The general structure of the closed-loop control system is depicted in Fig. 1. The LQG controller is a combination of a linear-quadratic regulator (LQR) state feedback and a Kalman filter state estimator. The LQG controller is tuned by selecting the LQR performance index weighting factors so that we optimally dispatch generators and controllable loads (in general, active-power injections $\Delta P[k]$). The LQG controller is optimal in the sense that the LQR state-feedback control law requires minimal active-power injection deviations (away from, e.g., the optimal economic dispatch solution) and the Kalman filter accounts for random system and measurement noise (i.e., $w[k]$ and $r[k]$, respectively), with which the power system naturally contends.

A. Linear-quadratic Regulator

The LQR optimal feedback control law is

$$\Delta P[k] = -K\left(P_{(m,n)}[k] - P^{\text{ref}}_{(m,n)}\right), \quad (15)$$

where the feedback gain K (and in turn, $\Delta P[k]$) is designed in order to minimize the quadratic cost function [8]

$$J = \sum_{k=0}^{\infty}\left((P_{(m,n)}[k] - P^{\text{ref}}_{(m,n)})^{\mathrm{T}}\Psi(P_{(m,n)}[k] - P^{\text{ref}}_{(m,n)})\right) + \sum_{k=0}^{\infty}\Delta P^{\mathrm{T}}[k]\Pi\Delta P[k] \quad (16)$$

subject to the constraints

$$P_{(m,n)}[k+1] = P_{(m,n)}[k] + \Phi_P[0]\Delta P[k], \quad (17)$$

$$0 = \mathbb{1}_N^{\mathrm{T}}\Delta P[k]. \quad (18)$$

In (16), $\Psi \in \mathbb{R}^{E\times E}$ (symmetric positive semi-definite) and $\Pi \in \mathbb{R}^{N\times N}$ (symmetric positive definite) are performance-index weighing matrices. Namely, Ψ specifies the cost of line active-power flows deviating away from their reference values, and Π embeds the cost of the control inputs, in our case, either generation output or controllable loads. The dynamical system in (17) follows from (13), where the contributions of each active-power nodal injection to the line active-power flows at the initial condition, i.e., $\Phi_P[0]$, are used. The equality constraint (18) enforces active-power balance at each time instant k. To systematically incorporate (18) and obtain a standard DT infinite-horizon LQR optimal control problem, we rewrite the quadratic cost function in (16) as follows:

$$J_K = \sum_{k=0}^{\infty}\left((P_{(m,n)}[k] - P^{\text{ref}}_{(m,n)})^{\mathrm{T}}\Psi(P_{(m,n)}[k] - P^{\text{ref}}_{(m,n)})\right) + \sum_{k=0}^{\infty}\Delta P^{\mathrm{T}}[k]\widetilde{\Pi}\Delta P[k] \quad (19)$$

where $\widetilde{\Pi} = (\Pi + \mathbb{1}_N\gamma\mathbb{1}_N^{\mathrm{T}})$ is a symmetric positive definite matrix, $\gamma \in \mathbb{R}^+$ (and generally larger compared to entries of Π). The cost function in (19) and constraint (17) are now in standard LQR form. Notice that the term $\Delta P^{\mathrm{T}}[k]\widetilde{\Pi}\Delta P[k]$ not only embeds the cost of control input (as in (16)) but also penalizes solutions that violate power balance.

In accordance with standard LQR design, $K \in \mathbb{R}^{N\times E}$ is the optimal state-feedback gain, given by [9]

$$K = \left(\widetilde{\Pi} + \Phi_P^{\mathrm{T}}[0]G\Phi_P[0]\right)^{-1}\Phi_P^{\mathrm{T}}[0]G. \quad (20)$$

Above, G is the unique positive definite solution of the discrete algebraic Riccati equation (DARE) described by [9]

$$\Psi - G\Phi_P[0]\left(\widetilde{\Pi} + \Phi_P^{\mathrm{T}}[0]G\Phi_P[0]\right)^{-1}\Phi_P^{\mathrm{T}}[0]G = 0. \quad (21)$$

As expressed in (20), K is computed only once using $\Phi_P[0]$ obtained at the initial condition. We could also choose to

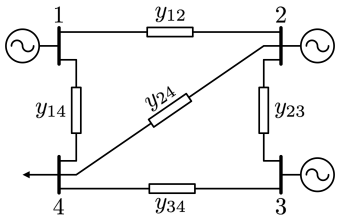

Fig. 2: Network topology for a 4-bus system.

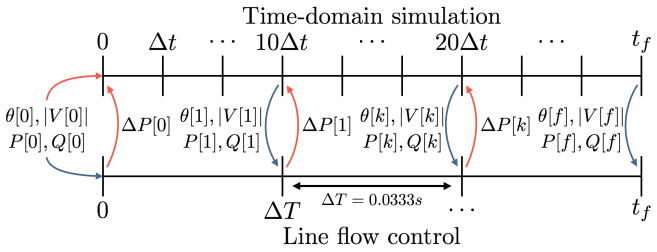

Fig. 3: Time-domain simulation and line flow control relative time scales.

reevaluate the feedback gain K at each time instant k with $\Phi_P[k]$. In practical implementation, we expect that K would be updated periodically as the operating point deviates further away from the initial conditions.

B. Kalman Filter

It is often preferable to use a constant estimation gain to simplify the implementation of the Kalman filter, which in most cases does not degrade the estimator performance. In light of this, the Kalman filter estimation law is chosen as

$$\widehat{P}_{(m,n)}[k+1] = \widehat{P}_{(m,n)}[k] + \Phi_P[k]\Delta P[k] + L(\overline{P}_{(m,n)}[k] - \widehat{P}_{(m,n)}[k]), \quad (22)$$

where $\widehat{P}_{(m,n)}[k]$ represents the state estimates, $\overline{P}_{(m,n)}$ is the measurement of the line flows, and L is the steady-state Kalman filter optimal gain. The optimal state-estimation gain is given by [9]

$$L = M\left(M + R_r\right)^{-1}, \quad (23)$$

where R_r denotes the measurement noise (i.e., $r[k]$) covariance. In (23), M is the unique positive definite solution for the Kalman filter DARE described by [9]

$$R_w - M\left(R_r + M\right)^{-1} M = 0, \quad (24)$$

where R_w denotes the covariance of $\Delta Q[k]$. With the L specified in (23), the DT steady-state Kalman filter minimizes the error covariance of the estimated states given by [8]

$$J_L = E\left\{(P_{(m,n)}[k] - \widehat{P}_{(m,n)}[k])^{\mathrm{T}}(P_{(m,n)}[k] - \widehat{P}_{(m,n)}[k])\right\}.$$

Based on the separation principle, the LQR state feedback control law and Kalman filter observer are designed separately and combined afterwards [9]. A DT infinite-horizon LQR control law is designed by specifying the weighting factors of the non-standard LQR cost function in (19). The cost function incorporates the power balance constraint to ensure feasibility of the injections at all times. As for the observer, a steady-state Kalman filter gain is obtained by incorporating random white-Gaussian disturbances and measurement noise in the system.

IV. Case Studies

This section illustrates the concepts developed in Sections II–III on a four-bus system with the one-line diagram shown in Fig. 2. Even though a power-flow model is used to design the LQG controller, it is verified with time-domain simulations of a full nonlinear differential-algebraic equation model accounting for synchronous generator dynamics. Throughout our case studies, PSAT is used to perform these time-domain simulations [10]. With respect to the 4-bus system in Fig. 2, synchronous generators, modelled with the classical model [11], are connected to buses 1, 2, and 3 and are initially injecting $P_1[0] = 0.426$ p.u., $P_2[0] = 1.1$ p.u., and $P_3[0] = 0.5$ p.u., respectively. A constant-power load is connected to bus 4, with active-power injection $P_4[0] = -2$ p.u. and reactive-power injection $Q_4[0] = -0.5$ p.u. The voltage magnitudes at buses 1, 2, and 3 are regulated to be $|V_1| = 1$ p.u., $|V_2| = 1$ p.u., and $|V_3| = 1$ p.u., respectively. Transmission lines are modelled using lumped parameters, where $y_{14} = y_{23} = y_{12} = 0.99 - \mathrm{j}9.9$ p.u., with $y_{12}^{\mathrm{sh}} = \mathrm{j}0.05$ p.u., and $y_{24} = y_{34} = 0.495 - \mathrm{j}4.95$ p.u. The resulting active-power flow on line $(1,4)$ is $P_{(1,4)}[0] = 0.834$ p.u.

Suppose that line $(1,4)$ supports a maximum active-power flow limit of 0.7 p.u. Thus, we wish to reduce its flow to $P_{(1,4)}^{\mathrm{ref}} = 0.7$ p.u. by specifying optimal active-power injections via the LQG-control framework introduced in Section III. We assume that the load at bus 4 must be served by the generators in the system, so the cost associated with varying the active-power injection at bus 4 is set to be exceedingly high. With this in mind, two scenarios are considered: (i) Case A—generator injection variations at buses 1, 2, and 3 have equal cost, and (ii) Case B—the cost of generation at bus 2 is lowered.

A. Equal Generator Costs

From the initial power-flow solution, we compute the nodal active- and reactive-power injection contribution factors using (11), with which the optimal feedback gain K is determined using (20) and the optimal state estimation gain L is computed using (23). With these control aspects in place, a time-domain simulation is performed to mimic the dynamic behaviour of the nonlinear system and is sampled at discrete intervals of $\Delta T = 0.0333$ s. This sampling time is realistic and well within the capability of current measurement technology [12]. As the bus voltages, angles, and nodal injections change throughout the transient response, the nodal active- and reactive-power injection contributions are recomputed at every time step. Then, leveraging the recomputed nodal injection contributions, the controller determines the optimal nodal active-power injection variations via $\Delta P[k] = -K(P_{(m,n)}[k] - P_{(m,n)}^{\mathrm{ref}})$, which serve as an input to the time-domain simulation. The interactions between

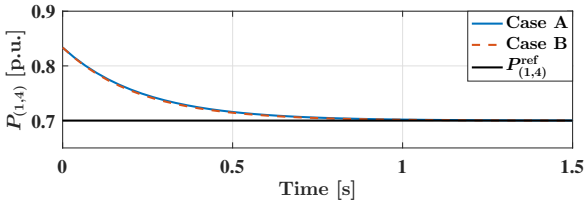

Fig. 4: Trajectory of active-power flow in line $(1, 4)$. The line flow converges to 0.7 p.u. as desired.

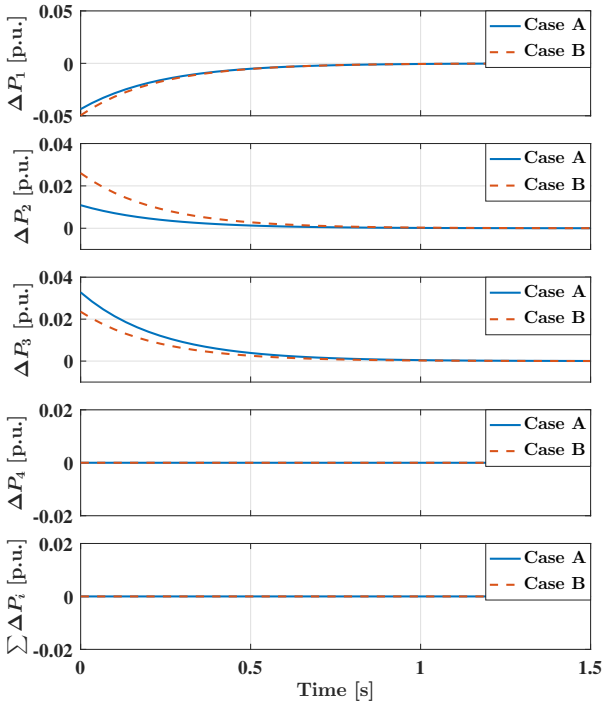

Fig. 5: Active-power injection variations and imbalances.

the time-domain and the line-flow controller simulations are illustrated in Fig. 3.

As shown in Fig. 4, the LQG controller behaves as expected and the active-power flow in line $(1, 4)$ indeed converges to the desired reference value of $P^{\text{ref}}_{(1,4)} = 0.7$ p.u. in less than 1 s. With respect to the active-power injections shown in Fig. 5, the cost of varying the load at bus 4, i.e., ΔP_4, is set to be exceedingly expensive whereas injection variations at other buses are equally priced. Due to its high price, as shown in Fig. 5, $\Delta P_4[k]$ remains at 0 throughout the simulation. The active-power injection imbalances are eliminated resulting in total active-power injection changes of $\Delta P_1 = -0.33$ p.u., $\Delta P_2 = 0.082$ p.u., $\Delta P_3 = 0.247$ p.u., and $\Delta P_4 = 0$ p.u.

B. Incorporating Different Generator Costs

For Case B, suppose that it is desirable to increase the active-power contribution of bus 2 due to a lower generation cost. This is achieved by lowering the weighting factor within the LQR formulation corresponding to ΔP_2. In this case, the load remains exceedingly expensive, and ΔP_1 and ΔP_3 remain equally priced, as in Case A. As shown in Fig. 4, similar to Case A, $P_{(1,4)}[k]$ converges to its desired reference value. The active-power injection variation at bus 2 increases due to its lower cost. In Fig. 5, the load remains unchanged and power balance is maintained throughout. For this case, the total active-power injection changes are $\Delta P_1 = -0.36$ p.u., $\Delta P_2 = 0.189$ p.u., $\Delta P_3 = 0.171$ p.u., and $\Delta P_4 = 0$ p.u.

V. Concluding Remarks

In this paper, we proposed a method for controlling active-power flows on transmission lines using LQG control. The main advantages of LQG control are intuitive tuning of design parameters, optimal trajectories regardless of disturbance size or initial conditions, and robustness against disturbance and measurement noise. The LQG controller dynamic performance and time response were demonstrated via case studies involving a 4-bus network. Compelling avenues for future work include decentralized implementations as well as applications in congestion management and the line reclosure problem.

References

[1] S. Ahmad, F. M. Albatsh, S. Mekhilef, F. Choudhury, A. A. Hossain, M. M. Hasan, and S. K. Nath, "Implementation of fuzzy unified power flow controller to control power flow dynamically in transmission line," in *2015 International Conference on Advances in Electrical Engineering (ICAEE)*, Dec 2015, pp. 271–275.

[2] S. R. Gaigowal and M. M. Renge, "Distributed power flow controller using single phase DSSC to realize active power flow control through transmission line," in *2016 International Conference on Computation of Power, Energy Information and Commuincation (ICCPEIC)*, Apr 2016, pp. 747–751.

[3] D. M. Divan, W. E. Brumsickle, R. S. Schneider, B. Kranz, R. W. Gascoigne, D. T. Bradshaw, M. R. Ingram, and I. S. Grant, "A distributed static series compensator system for realizing active power flow control on existing power lines," *IEEE Transactions on Power Delivery*, vol. 22, no. 1, pp. 642–649, Jan 2007.

[4] S. C. Mller, U. Hger, and C. Rehtanz, "A multiagent system for adaptive power flow control in electrical transmission systems," *IEEE Transactions on Industrial Informatics*, vol. 10, no. 4, pp. 2290–2299, Nov 2014.

[5] L. Gyugyi, "Unified power-flow control concept for flexible AC transmission systems," *Generation, Transmission and Distribution, IEEE Proceedings C*, vol. 139, no. 4, pp. 323–331, Jul 1992.

[6] Y. Zhang, L. Dong, and Z. Gao, "Load frequency control for multiple-area power systems," in *2009 American Control Conference*, Jun 2009, pp. 2773–2778.

[7] Y. C. Chen and S. V. Dhople, "Power divider," *IEEE Transactions on Power Systems*, vol. 31, no. 6, pp. 5135–5143, Nov 2016.

[8] M. Athans, "The role and use of the stochastic linear-quadratic-gaussian problem in control system design," *IEEE Transactions on Automatic Control*, vol. 16, no. 6, pp. 529–552, Dec 1971.

[9] A. Kalbat, "Linear quadratic gaussian (LQG) control of wind turbines," in *Electric Power and Energy Conversion Systems (EPECS), 2013 3rd International Conference on*, Oct 2013, pp. 1–5.

[10] F. Milano, "An open source power system analysis toolbox," *IEEE Transactions on Power Systems*, vol. 20, no. 3, pp. 1199–1206, Aug 2005.

[11] P. M. Anderson and A. A. Fouad, *Power system control and stability*. John Wiley & Sons, 2008.

[12] US DOE & FERC. (2006, Feb) Steps to establish a real-time transmission monitoring system for transmission owners and operators within the eastern and western interconnections. [Online]. Available: http://energy.gov/sites/prod/files/oeprod/DocumentsandMedia/final_1839.pdf